Impedance analysis of cultured cells: A mean-field electrical response model for electric cell-substrate impedance sensing technique

E. Urdapilleta, M. Bellotti, and F. J. Bonetto*
Laboratorio de Cavitación y Biotecnología, Instituto Balseiro, CAB/CNEA, 8400 S.C. de Bariloche, RN, Argentina
(Received 16 November 2005; published 9 October 2006)

In this paper we present a model to describe the electrical properties of a confluent cell monolayer cultured on gold microelectrodes to be used with electric cell-substrate impedance sensing technique. This model was developed from microscopic considerations (distributed effects), and by assuming that the monolayer is an element with mean electrical characteristics (specific lumped parameters). No assumptions were made about cell morphology. The model has only three adjustable parameters. This model and other models currently used for data analysis are compared with data we obtained from electrical measurements of confluent monolayers of Madin-Darby Canine Kidney cells. One important parameter is the cell-substrate height and we found that estimates of this magnitude strongly differ depending on the model used for the analysis. We analyze the origin of the discrepancies, concluding that the estimates from the different models can be considered as limits for the true value of the cell-substrate height.

DOI: 10.1103/PhysRevE.74.041908 PACS number(s): 87.80.−y, 87.17.−d, 87.18.−h

I. INTRODUCTION

Tissue culture has allowed the study of cellular behavior to extend due to, among other things, the better reproducibility of experimental conditions and the ease of running experiments. Many of the properties and functions that different animal cells show when they are part of a tissue in a living being are believed to remain intact in *in vitro* cultures in the current state of art [1]. Consequently, *in vitro* experiments concerning these properties and functions are valuable.

The electric cell-substrate impedance sensing (ECIS) technique, which shows to be extremely sensitive and versatile, evaluates, in a noninvasive fashion, morphological and functional properties of a cellular set. This technique, developed by the pioneer work of Giaever and Keese (G&K), is based on the growth of adherent cells on a biocompatible substrate in which there are small gold electrodes that sense the properties and functions of the cells as a whole through an electrical measurement. As cells attach and spread on the electrode, the impedance of the system counter-electrode/medium/cells-monolayer/collector-electrode changes. The way the impedance changes gives information about the morphological characteristics of the cells, the development of junctions between neighboring cells, and the strength of the adhesion to the substrate. Details of this technique can be found in Refs. [2–5].

Due to the characteristics of the ECIS technique, it is possible to carry out an increasing number of experiments. The versatility of the technique is apparent in the wide variety of studies in which it has been applied: the monitoring of cell spread and adhesion in real time [2–6] and the different affinity that cells show when they are cultured in a medium supplemented with different adhesion proteins and, therefore, the additional evidence regarding the anchorage mechanism responsible of the attachment in such cells [6]; the observation of cellular micromotion and its characterization as a parameter of metabolic health [4,5,7,8]; the quantitative evaluation of the harmful effects produced by particular compounds in a variety of cells cultured *in vitro* [9,10]; the assessment of structural changes associated with different cellular processes, such as apoptosis or signal transduction pathways, elucidated by the presence of particular substances when certain cells are involved [11–15]; the measurement of the barrier function of confluent monolayers and the elucidation of different aspects related with this function [16–19]; the monitoring of the metastatic process occurring when different metastatic cells invades a culture of endothelial cells [20]; the study of the cell response to either physical [21–23] or chemical [12–15,24] changes; and the electroporation of cellular membranes or even the cell destruction by means of electrical impulses and the posterior study of the associated wound-healing/migration phenomenon [25,26], among many other studies that the technique makes possible [27]. The most outstanding characteristic of the technique is its potential in all experiments involving morphological changes and formation of cell-cell and cell-extracellular matrix interactions because, as it has been proved, they are fundamental processes in much of the most essential current research in biology and medicine such as cellular differentiation, inflammation processes, or tumor growth.

One of the main characteristics of the ECIS method is that it is possible to analyze temporal responses of cells cultured in different conditions. In addition, the complete electrical response of the system is contained, for every instant in time, in the behavior of the in-phase and out-of-phase voltages, with respect to the excitation wave, or the resistance and capacitance in an in-series equivalent circuit, for all frequencies. Then, in every instant, the complete response is a frequency scan. Afterwards, frequency domain data can be processed by means of different models to obtain electrical as well as morphological characteristics of the system under study, such as the intercellular electrical resistance or the membrane capacitance. Particularly, with the G&K model [7], the height between the substrate and the basal membrane

*Corresponding author. Electronic address: bonetto@ib.edu.ar

of a cell can be inferred. Recently, particular interest has been focused on this magnitude for two reasons. Firstly, many studies have required the inference of the cell-substrate height to analyze other properties of the cells [17,19,22,23], and the ECIS technique has been chosen for this purpose. Secondly, signal measurement of systems containing active biological elements (neurons, for instance) is strongly related to seal resistance, which is defined by the cell-substrate height [28].

In this paper, we report on a model for the analysis of the electrical response of monolayers cultured *in vitro* that, by adjusting data of a typical ECIS experiment, gives, among others, the mean cell-substrate height. We found the estimate for this parameter strongly differs from that obtained with the G&K model. We discuss the origin of this discrepancy, and conclude on the proper interpretation of its estimates. Additionally, based on this parameter, we are able to evaluate each model considered, distributed as well as lumped parameters models.

II. THEORY

A. Electrical response models of cell-covered electrodes

The electrical behavior of an electrode in contact with an electrolyte (culture medium) has been extensively studied [29,30]. When cells are cultured on a microelectrode, the electrical response of the system microelectrode-cells/medium changes with respect to the response in the absence of cells. This is valid whether the cells are arranged in a monolayer or not, as well as for cells being in confluence or not. Such a system presents specific electrical properties that can be established from the spectral response of the system impedance. This kind of determination is performed either by the ECIS technique (electric cell-substrate impedance sensing) or by a related one. Through this technique, the in-series equivalent resistances and capacitances of the system can be measured. However, the analysis of the data requires the formulation of a model that relates the electrical response with properties of the cells.

The current models for the interpretation of the electrical response of a cell monolayer cultured on appropriate electrodes can be classified into two distinct approaches: one that considers the electrical properties as lumped parameters and another based on microscopic characteristics of the monolayer.

Under the first approach, it is assumed that the microscopic characteristics of the system, such as the properties associated with the cell membranes or the development of tight junctions in different cellular types, create global electrical properties for the ensemble of cells. In this kind of model, an explicit dependence on the position for any of the involved magnitudes (e.g., the current flowing under the monolayer) does not exist and such dependences could be considered averaged over the whole electrode. Once this hypothesis has been accepted and depending on the particular characteristics of the cellular line, different schemes are proposed for the lumped parameter circuit associated to the monolayer [13,31–33]. Among these, the simplest circuit is a *RC* element, which consists of the parallel arrangement of a resistance R_p and a capacitance C_p representing, respectively, the ionic permeability of the monolayer and the transcellular current transport characteristics, both considered as independent phenomena [31].

Under the second approach, we can include the tight epithelium formulation due to Clausen *et al.* [34], the G&K original model [7] used to analyze the results provided by the ECIS technique, and the subsequent improvement made by Lo *et al.* [35,36] based on the underlying ideas of both prior models. In all these models, the electrical response in the presence of a cell monolayer is caused by the inherent distributed effects of the system under study. Such a response can be obtained by means of the analysis of the electrical behavior in cellular units, coupled through suitable boundary conditions.

In the following paragraphs, we review in some detail the model proposed by G&K [7]. This model is based on the fact that the cell monolayer geometrically blocks the current flow with respect to the current flow measured in absence of cells (naked response). Between the electrode surface and the bottom of the cells there is a space occupied by the electrolyte. This space is implicitly assumed to be larger than a few nanometers, and therefore, even in the presence of cells, the electrical behavior of the current flowing through the electrode in contact with the electrolyte is analogous to the behavior of the naked electrode. Once it crosses the electrode-medium interface, the current flows following different paths. The relative importance of the different paths depends on the specific impedances that are developed by the monolayer attached to the electrode. This model proposes that there can be two paths: either between the substrate-cell space or through the cell membrane.

In a simplified manner, the resistance produced by the cellular monolayer is due to the current passage underneath cells (distributed effect) and the current passage crossing intercellular spaces, through a junction resistance (lumped effect). The current that directly crosses the cell presents an essentially capacitive behavior.

As we said before, in this kind of approach, the analysis in a cellular unit provides the system response in the presence of cells. In this sense, cells are represented as circular disks of radius r_c and the analysis is carried out up to the one cell limit where a proper boundary condition is imposed. Figure 1 shows the outstanding variables in the current distribution, the drops in potential developed in the system and the volume utilized for the integral analysis. Electrical properties are considered by both the specific impedance of the naked electrode, $Z_n(\omega)$ [37], and the specific impedance due to the presence of cells (basically, the impedance of two cellular membranes connected in series considering that each of both membranes only shows a capacitive behavior), $Z_m(\omega)$.

Based on different balances, which are related to drops in potential and conservation of current, an ordinary differential equation of second order for the potential developed in the cell-substrate space, V, can be obtained,

$$\frac{d^2V}{dr^2} + \frac{1}{r}\frac{dV}{dr} - \gamma^2 V + \beta = 0, \tag{1}$$

where

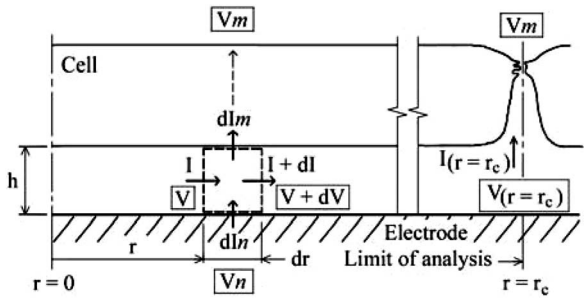

FIG. 1. Giaever and Keese Model. The cell is represented by a circular disk of radius r_c and there is a space of height h between the substrate and the cell. The current going out the electrode, I_n, distributes in one of two directions: part of the current flows in a radial direction, I, and the remaining current directly crosses the cell, I_m. The drops in potential for the system are described by the applied potential, V_n, the potential in the electrolyte bulk, V_m, and the potential in the cell-substrate space, V. In the end of the cell, $r=r_c$, there is a tight junction between neighbor cells functioning as an electrical resistance (lumped effect).

$$\gamma^2 = \frac{\rho}{h}\left[\frac{1}{Z_n} + \frac{1}{Z_m}\right],$$

$$\beta = \frac{\rho}{h}\left[\frac{V_n}{Z_n} + \frac{V_m}{Z_m}\right]. \tag{2}$$

Because of the geometry assumed for the cell, the formulation is simplified when expressed in cylindrical coordinates. Above, ρ is the known resistivity of the medium, h is the height of the cell-substrate space, V_n is the applied potential, and V_m is the potential beyond the monolayer.

The general solution of the Eq. (1) is given by

$$V = C_1 I_0(\gamma r) + C_2 K_0(\gamma r) + \frac{\beta}{\gamma^2}, \tag{3}$$

where I_0 and K_0 are the modified Bessel functions of first and second kind, respectively, of zero order.

Because K_0 diverges at the origin, the constant C_2 must be zero. The constant C_1 is determined with the boundary condition

$$V_{(r=r_c)} - V_m = \frac{R_b}{\pi r_c^2} I_{(r=r_c)}, \tag{4}$$

where I is the current in the cell-substrate space and R_b is a resistance (by unit area) due to the formation of intercellular junctions. This condition implies that the potential drop at the end of the cell can be considered as a lumped effect. The current under the cell that reaches its boundary cannot cross the limit of the system because the neighboring cell is identical to the cell under study; thus, by symmetry, in this region the current must axially cross the cells through a tight junction that acts electrically as a resistance. This type of analysis by unit cells is justified when all cells are equivalent. In such cases, the boundary condition (restricting the analysis to only one cell) results are simple, such as in the model described in this section. However, the region studied, rigorously, is not a unit cell because it does not fill the space. In this analysis, there are spaces between consecutive regions that are not considered within any region. Nevertheless, this is a minor concern since, according to Ref. [7], the results obtained under this formulation agree with those obtained with a formulation based on regions of rectangular base which does fill the space.

Once the constants are determined, the variables of the system are defined and so, the specific impedance of the cell-covered electrode can be established, which is given by

$$\frac{1}{Z_{\text{cov}}} = \frac{1}{Z_n}\left[\frac{Z_n}{Z_n + Z_m} + \frac{\dfrac{Z_m}{Z_n + Z_m}}{\dfrac{\gamma r_c}{2}\dfrac{I_0(\gamma r_c)}{I_1(\gamma r_c)} + R_b\left(\dfrac{1}{Z_n} + \dfrac{1}{Z_m}\right)}\right], \tag{5}$$

where

$$\alpha = r_c\sqrt{\frac{\rho}{h}}. \tag{6}$$

This model has then two adjustable parameters: α and R_b. A greater complexity can be achieved by considering the specific impedance through the cells, $Z_m(\omega)$, as a capacitive impedance with the particular value of the capacitance becoming an additional parameter.

B. A mean-field model

Combining elements from the two approaches used for the analysis of the electrical response in presence of cells, an alternative approach can be established.

In the formulation by unit cells due to G&K, the magnitudes involved inside the volume under analysis are extended periodically over the other units as far as infinity. Figure 2(a) shows the suggested configuration for one of the significant magnitudes. By considering the cell size as a fixed magnitude, the analysis results are appropriate when the electrode is large enough to be covered by several cells.

When the dimension of the electrode is in a range that both registers the collective behavior (greater than a few cells' size) but it is not large enough to be considered infinite, the electrical response in the electrode is also influenced by the behavior imposed by its finite extension. The electrodes used in ECIS experiments are in this range (except those utilized by Wegener *et al.* [31], which are a few millimeters in size and, therefore, can be considered infinite). By extending the G&K model so that the whole electrode may be considered the volume under analysis, we can obtain a differential equation similar to Eq. (1) for the cell-substrate potential. Scaling up the situation in Fig. 2(a), this potential for the entire electrode satisfies a relationship as it is shown in Fig. 2(b), performing a kind of modulation where the microscopic response due to each individual cell is mounted over it.

The model we present is based on the hypothesis that this macroscopic behavior, obtained from an extended microscopic analysis, dominates the overall electrical response of the cell-covered electrode. Additionally, cells lose their individual condition: the electrical response is modified because of the existence of a monolayer showing definite mean elec-

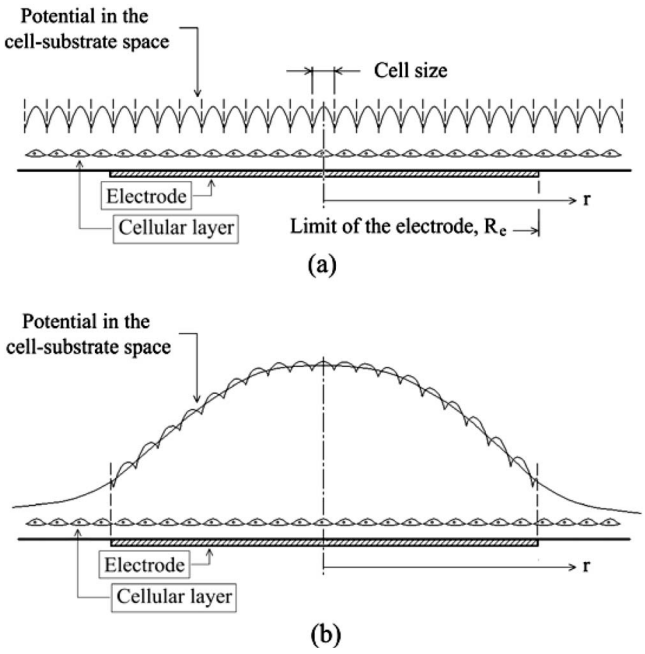

FIG. 2. Potential in the cell-substrate space. (a) In the G&K model, the potential described in one unit cell is repeated up to infinite. (b) When the finite size of the electrode is considered, there is an overall behavior performing a modulation of the microscopic response.

trical properties (due to the particular arrangement of the cells), which are measured by the specific impedance of the monolayer, $Z_{cells}(\omega)$. Unlike the electrode, the monolayer can be considered to extend up to infinity. Consequently, and because cells lose their individual condition, any point in the monolayer observes the same environment. Therefore, Z_{cells} is an independent-position value. This is a valid condition for complete monolayers, even though they may not be in a confluence state, but have a simply connected topology (without holes). The model shares the remaining hypotheses with the G&K model.

The current crossing the electrode flows into two pathways: in the radial direction and through the cellular layer. In this model, the radial flow of current under analysis extends beyond the end of the electrode even though there is not a current supply once the limit of the electrode is crossed. Finally, all of the current crosses the layer. This situation is schematically shown in Fig. 3.

There are two regions to be considered: the region inside the limits of the electrode and the region outside. Consequently, two independent balances must be developed, one for each region, and then coupled by means of appropriate boundary conditions in the common border. Figure 4 shows the variables involved in the model, the drops in potential that appear, and the volumes utilized for the integral analysis.

The balances in each region are analogous to the balance in the G&K model; therefore, the equations describing the potential behavior in the cell-substrate space are given by

$$\frac{d^2V_{rad}^{in}}{dr^2} + \frac{1}{r}\frac{dV_{rad}^{in}}{dr} - \gamma_{in}^2 V_{rad}^{in} + \beta_{in} = 0, \quad r < R_e, \tag{7}$$

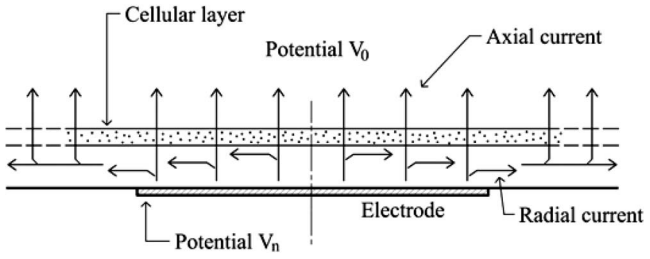

FIG. 3. Distribution of the current in the proposed model. The current that crosses the electrode distributes either in a radial direction or in an axial direction crossing the cellular layer.

$$\frac{d^2V_{rad}^{out}}{dr^2} + \frac{1}{r}\frac{dV_{rad}^{out}}{dr} - \gamma_{out}^2 V_{rad}^{out} + \beta_{out} = 0, \quad r > R_e, \tag{8}$$

where R_e is the radius of the electrode and

$$\gamma_{in}^2 = \frac{\rho}{h}\left(\frac{1}{Z_n} + \frac{1}{Z_{cells}}\right),$$

$$\gamma_{out}^2 = \frac{\rho}{h}\frac{1}{Z_{cells}},$$

$$\beta_{in} = \frac{\rho}{h}\left(\frac{V_n}{Z_n} + \frac{V_0}{Z_{cells}}\right),$$

$$\beta_{out} = \frac{\rho}{h}\frac{V_0}{Z_{cells}}. \tag{9}$$

Like the G&K model, this analysis also considers that the specific impedance of the naked electrode, $Z_n(\omega)$, as well as the resistivity of the medium, ρ, are known. However, the specific impedance of the monolayer, $Z_{cells}(\omega)$, replaces the in-series impedance of the cellular membranes in the G&K model, $Z_m(\omega)$.

The general solutions of the Eqs. (7) and (8) are similar to Eq. (3),

$$V_{rad}^{in} = C_1^{in} I_0(\gamma_{in} r) + C_2^{in} K_0(\gamma_{in} r) + \frac{\beta_{in}}{\gamma_{in}^2}, \quad r < R_e, \tag{10}$$

$$V_{rad}^{out} = C_1^{out} I_0(\gamma_{out} r) + C_2^{out} K_0(\gamma_{out} r) + \frac{\beta_{out}}{\gamma_{out}^2}, \quad r > R_e. \tag{11}$$

For the solution inside the electrode, V^{in}, we must consider that the Bessel function $K_0(\gamma_{in} r)$ diverges at the origin, so C_2^{in} must be zero. For the solution outside, V^{out}, this potential finally reaches the potential in the electrolyte bulk, V_0,

$$V_{rad}^{out}(r \to \infty) = V_0. \tag{12}$$

The two remaining boundary conditions must be specified in the common border to the regions, $r = R_e$ through the continuity requirement for both the potential and the current,

$$V_{rad(r=R_e)}^{in} = V_{rad(r=R_e)}^{out},$$

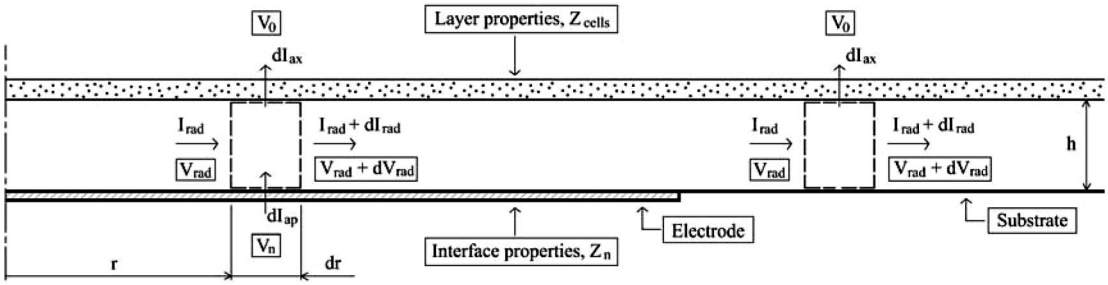

FIG. 4. Proposed model. Inside the electrode, the current that crosses it, I_{ap}, distributes radially, I_{rad}, and axially, I_{ax}, in the cell-substrate space of height h. Outside the electrode, a current supply from the substrate does not exist. The drops in potential are represented by the applied potential, V_n, the potential in the electrolyte bulk, V_0, and the potential in the cell-substrate space, V_{rad}.

$$I^{in}_{rad(r=R_e)} = I^{out}_{rad(r=R_e)}. \tag{13}$$

By means of the relations that are established in the different balances, the continuity requirement for the current can be replaced by

$$\left.\frac{dV^{in}_{rad}}{dr}\right|_{r=R_e} = \left.\frac{dV^{out}_{rad}}{dr}\right|_{r=R_e}. \tag{14}$$

Operating with these four boundary conditions, and by considering that [38]

$$V_n - V_0 = \frac{Z_{\mathrm{cov}}}{\pi R_e^2} I_{ap}, \tag{15}$$

where

$$I_{ap} = \int_0^{R_e} \frac{2\pi r}{Z_n}(V_n - V_{rad})dr, \tag{16}$$

the specific impedance for the cell-covered system, Z_{cov}, can be obtained,

$$\frac{1}{Z_{\mathrm{cov}}} = \frac{1}{Z_n}\left\{\frac{Z_n}{Z_n + Z_{cells}} + \frac{\dfrac{Z_{cells}}{Z_n + Z_{cells}}}{\dfrac{\gamma_{in}R_e}{2}\left[\dfrac{I_0(\gamma_{in}R_e)}{I_1(\gamma_{in}R_e)} + \dfrac{\gamma_{in}}{\gamma_{out}}\dfrac{K_0(\gamma_{out}R_e)}{K_1(\gamma_{out}R_e)}\right]}\right\}. \tag{17}$$

At this stage, the proposed model does not have much usefulness since the dependence on the frequency for the specific impedance of the monolayer, $Z_{cells}(\omega)$, is unknown. To obtain some useful information from the system, we must model the electrical behavior of the monolayer. For this purpose, the approach presented first becomes important; point-to-point (in a macroscopic perspective), the simplest way to consider the monolayer with models of lumped parameters is through an in-parallel arrangement composed by a resistance and a capacitance [39]. With this approximation, we have

$$\frac{1}{Z_{cells}} = \frac{1}{R_{cells}} + i2\pi f C_{cells}. \tag{18}$$

Thus, the model includes three adjustable parameters: R_{cells}, C_{cells}, and ρ/h.

III. MODEL VALIDATION, RESULTS, AND DISCUSSION

We compared experimental and fitted data, obtained with the different models, for the response of the MDCK (Madin-Darby Canine Kidney) cell line, which is commonly used in ECIS experiments for impedance analysis.

A. Electrodes and instrumentation

Scan frequency data obtained with ECIS technique require multiple measurements of in-phase and out-of-phase voltages at different frequencies. Typically, the setup consists of a wave-form generator, a lock-in amplifier, a computer, and the electrodes [2], schematically connected as it is shown in Fig. 5. The main differences in our setup with respect to a classical ECIS one are the use of a DSP-based lock-in, and the use of a resistive divisor (see Wegener *et al.* [31]). DSP-based lock-in was developed in our laboratory [40], and it performs the wave generator and amplifier functions simultaneously. Basically, it consists of a general purpose DSP unit (digital signal processor) programmed to operate as a lock-in, digitally multiplying the reference and the signal, while it sends a controlled output. On the other hand, to set the proper scale for the electrical stimulation, we used a resistive divisor which becomes a constant voltage source (instead of a constant ac current source [2,31]) for the signal feeding the experiment. Due to this configuration and to the electrical impedances used in the setup, we had to perform some simple calculations to obtain the resistance and capacitance of the system under study at each frequency of excitation. With appropriate resistances in the divisor, point *A* in Fig. 5 always developed a constant voltage independently of the impedances in the system under study (either naked or covered electrode impedance). The signal at point *A* fed the experiment in series to a resistance R_s, which guaranteed the divisor worked properly. The in-phase and out-of-phase potentials were measured with the DSP-based lock-in amplifier referenced with its output signal.

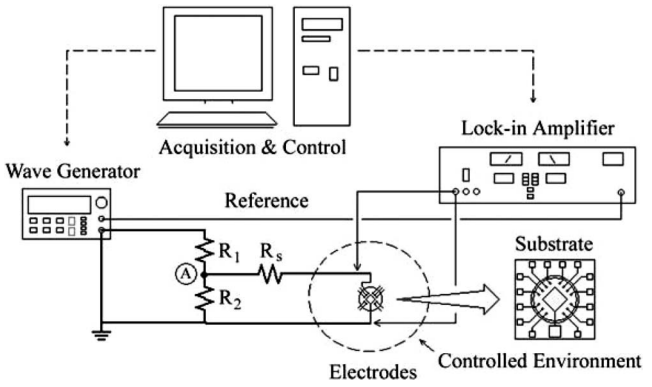

FIG. 5. Schematic of the experimental setup used for impedance measurements. Electrodes are built and treated as described in Sec. III A, and placed in a controlled environment. A wave generator (WG) feeds a resistive divisor, where $R_1=1.0$ kΩ and $R_2=10$ Ω. A resistance, $R_s=15$ kΩ, connected in-series to the experiment, ensures a fixed value for the potential at point A, whatever the impedance developed by the system under study. In-phase and out-of-phase drops in potential produced in the electrode are registered by a lock-in amplifier, phase-locked to the WG. Both the WG function and the lock-in function are performed by a DSP-based lock-in amplifier controlled by a computer, which in turn also collects electrical data.

The electrodes were built with a similar procedure as described by Giaever & Keese [2]. A 100 nm layer of gold was sputtered on the substrate, a 25 mm$\times$25 mm slice of glass, and then covered with a layer of photoresist (Shipley 1818), approximately 3 μm thick, by spinning and baking. Using standard photolithography techniques, we delimited the electrode shapes with a proper mask. Then, the gold exposed on the substrate was etched with royal water. The electrodes were formed by the remaining gold on the substrate, and the photoresist protecting them was diluted in acetone. The geometry used consisted of a large diamond-shaped counter electrode connected to signal ground, and several circular-shaped electrically independent electrodes of sizes in the order of 500 μm. These small electrodes were connected to the DSP-based lock-in input. In order to reduce the alterations present in the neighborhood of the cells, we did not use photoresist or any other electrical insulator. With this configuration, the cells were in contact only with either glass or gold. Thus the response was produced in a parallel connection between an electrode of 500 μm diameter and its electrical strip 50 μm wide. A glass cylinder of approximately 10 mm internal diameter and 10 mm length was glued with epoxy (Poxipol) to the glass substrate. The cylinder acted as a micro Petri dish containing the culture medium and the cells. Then, the substrate with the electrodes and the cylinder was glued to the base of a 90 mm diameter Petri dish, the gold leads were electrically connected to wires with silver paint, and the wires glued with epoxy to the base of the Petri dish.

B. Cell culture

A MDCK (Madin Darby Canine Kidney) cell line was obtained from the Banco Argentino de Células (Argentine Cells Bank), and cultured under standard conditions at 37 °C in a humidified incubator containing 5% CO_2. Dulbecco's modified eagle medium (DMEM F-12, Gibco) was used as culture medium, and was supplemented with 10% of bovine fetal serum, 1% antibiotic-antifungus solution (penicillin, streptomycin, fungizone), Hepes buffer, and 1% L-Glutamine. The culture medium was changed approximately twice a week and once in confluence, cell suspensions were prepared using standard trypsination procedures [0.05% (w/v) trypsin –0.53 mM EDTA·4Na]. Suspensions were done both for subcultivation purposes and for electrical properties measurements [1].

Electrodes were sterilized in an oven at 130 °C for approximately 2 h. They were also incubated with serum for 2–10 h before seeding the cells for the measurements. Proteins existing in the serum pretreated the electrode surface, enhancing the attachment of cells. Electrodes were seeded with 0.5 ml of cell suspension, 2.0×10^5 cells/ml, and were incubated for at least 24 h before measurements of cells in confluence were conducted. This condition was checked under microscope.

C. Electrical impedance results of MDCK cells in confluent monolayers

Previously, Lo *et al.* [35] and Wegener *et al.* [31] obtained electrical impedance results in confluent MDCK cells with the ECIS technique, but they analyzed their data with different models. In order to evaluate the different models, we measured the electrical characteristics of cellular monolayers of MDCK cells cultured on gold electrodes prepared as was described in the previous section. Figure 6 shows a typical result for a scan in a log-log scale of 100 frequency points obtained with the procedure described above (not all data points are shown), where the horizontal axis indicates the frequency of stimulation (20–20 000 Hz [41]) and the vertical axes indicate, respectively, the in-series resistance, and the in-series capacitance, for both naked and covered electrodes. The data fit for the three models considered is also shown, the G&K model, a *RC* parallel element such as the analysis by Wegener *et al.* [31], and our model with Z_{cells} modeled as a *RC* element, Eq. (18). To adjust the data, we used the Levenberg-Marquardt method (LM method) for nonlinear parameter estimation under each model [42]. In order to take into account that each frequency point f_i has two associated properties to be quantified [43], the merit function χ^2 to be minimized was calculated as

$$\chi^2(\vec{a}) = \sum_{i=1}^{N} \left\{ \left[\frac{R_i - R_{\mathrm{mod}}(f_i;\vec{a})}{\sigma_{R_i}} \right]^2 + \left[\frac{C_i - C_{\mathrm{mod}}(f_i;\vec{a})}{\sigma_{C_i}} \right]^2 \right\},$$

where $\bar{a}$ represents the set of parameters of the model considered, R_i and C_i are the properties measured at frequency f_i, σ_{Ri} and σ_{Ci} quantify the dispersion of the measurements in both magnitudes, and R_{mod} and C_{mod} are the properties calculated with the model for each frequency f_i based on the particular parameters $\bar{a}$.

As it was pointed out by Wegener *et al.* [31], the spread resistance [44] can change between the naked and the cov-

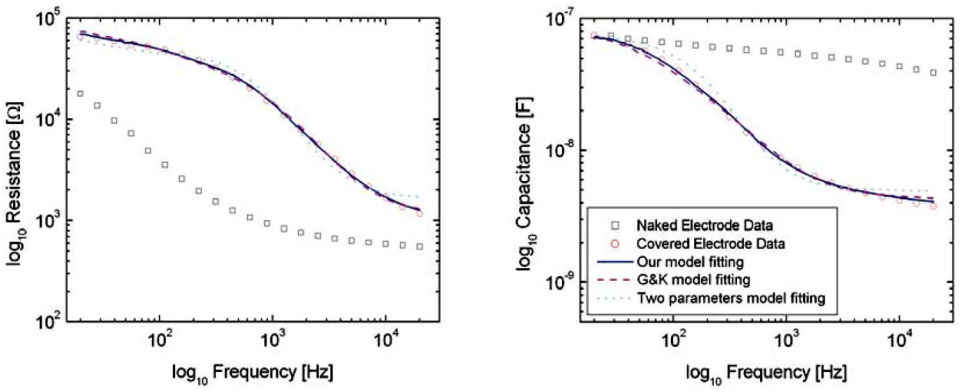

FIG. 6. (Color online) Electrical properties data for confluent MDCK cells cultured on gold electrodes. Squares indicate naked electrode response and circles indicate cell-covered electrode response. The vertical axes are the in-series equivalent resistance and capacitance for the system. Solid, dashed, and dotted lines are the properties calculated with our model, the G&K model, and the two-parameters model with the respective values of best fitting parameters obtained with LM method.

ered electrode, and therefore it is susceptible to being adjusted. Table I shows the best fitting parameter values obtained with the LM method for data shown in Fig. 6 for the three models considered.

The values we obtained for the parameters in the G&K model and the two parameters model are in good agreement with published reports [31,35]. As shown in Table I, by comparing the respective values of the merit function χ^2, we can see that G&K model is approximately as realistic as our model, when both have the same number of parameters [45]. The analysis used by Wegener *et al.* has a higher value of χ^2 but, since it has fewer parameters, it still could be considered as a good model for the system (given two models with the same value of χ^2, the fewer the parameters, the higher the evidence for a particular model). Table I shows that the different models give different values for the electrical parameters (parameters II and III) of the system. Regarding the cell-substrate height (α in the G&K model and ρ/h in our model), it should be noticed that each model gives extremely different values for this magnitude. By considering a given value for the cell radius [35], $r_c=7.0$ μm, the parameter ρ/h resulting from G&K model [see definition of α, Eq. (6)] is 1.4 GΩ. Then, the parameter shared between the G&K model and our model differs in three orders of magnitude, with this set of data. With an independent technique, Braun and Fromherz [46] estimated a magnitude equivalent to ρ/h in isolated MDCK cells. The value they estimated for this parameter was 9.3 MΩ, an intermediate value between those obtained here with the models utilized for ECIS data analysis. To gain insight into the physical meaning of the particular values, we can explicitly obtain the cell-substrate height by considering the resistivity of the medium in the cell-substrate space as the resistivity of cell culture medium, $\rho=54$ Ω cm. Under this assumption, the mean height results to be 0.38 nm in the G&K model and 1.0 μm in our model [47]. Clearly, the value obtained from the G&K model lies below the continuum limit (in addition, it does not seem plausible that there could be any protein in such a small space), and the value obtained from our model is physically so high that, for example, no trypsination process would be necessary to separate cells from the substrate (a situation that anybody working with this kind of cells can testify does not occur).

To address the discordance between the height estimation of these two models and relate each of them with the two-parameters model (which does not have any information about the cell-substrate height), we can think of a situation in which we analyze the behavior of one model at time, for cases where ρ/h behaves as the other model predicts.

Figures 7(a) and 7(b) show the normalized electrical properties [48] of the system calculated with our model based on the best estimation of the electrical parameters with the LM method for a fixed ρ/h, for different values of this parameter. The figures also show the calculated properties resulting from the overall best estimation (corresponding to the values cited in Table I) for our model and the two-parameters

TABLE I. Nonlinear parameter estimation with LM method for data shown in Fig. 3. All parameters estimations included an independent adjustment in the spread resistance.

	G&K Model	Two-Parameters Model	Mean-Field Model
χ^2	167	1240	71.5
Parameter I	$\alpha=26.3$ $\Omega^{1/2}$ cm	—	$\rho/h=0.533$ MΩ
Parameter II	$R_b=53.6$ Ω cm^2	$R=102$ Ω cm^2	$R_{\text{cells}}=301$ Ω cm^2
Parameter III	$C_m=1.966$ μF/cm^2	$C=2.271$ μF/cm^2	$C_{\text{cells}}=1.641$ μF/cm^2

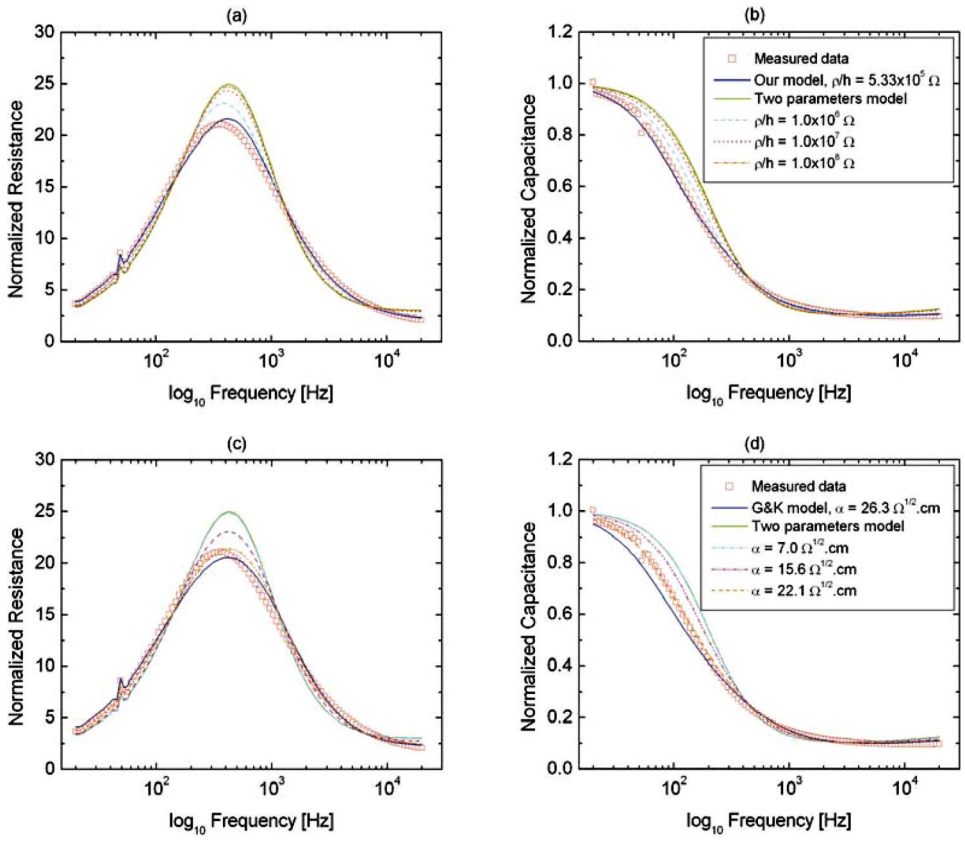

FIG. 7. (Color online) Normalized electrical properties of the system assuming a given value for the cell-substrate height, h, and minimizing χ^2 with the LM method. (a), (b) Properties calculated by this procedure under our model for different values of ρ/h. (c) and (d) Properties calculated under G&K model for different values of α. It is also shown the overall best fitting (data in Table I) for the corresponding models and the lumped parameters model.

model. We can see that the higher the assumed values for ρ/h, the closer the values of the two electrical parameters of this model are with respect to those estimated by the lumped parameters model. In particular, when ρ/h approaches the value estimated from the parameter α obtained with the G&K model, the in-series equivalent resistance and capacitance of the cell-covered electrode given by our model and the lumped parameter model are approximately equal. So, a close distance such as the one predicted by the G&K model reduces our model to the lumped parameters model. In other words, macroscopically, a height as low as the one predicted by the G&K model reduces the mean-field model to a two-parameter model.

Figures 7(c) and 7(d) show the normalized electrical properties calculated with a similar procedure for the G&K model, for different values of the parameter α fixed. Here, the limiting case is obtained in the opposite direction, when α is reduced from the value obtained with the best parameter estimation (Table I). Again, when in the model analyzed here (G&K model), the height predicted by the other model (mean-field model) (α=0.511 $\Omega^{1/2}$ cm) is imposed, the response approximates that resulting from the two-parameter model. Therefore, G&K model reduces to a lumped parameter model if a height as high as that predicted by our model were correct. Microscopically, a higher space reduces the behavior to one that can be modeled by only two parameters.

Figure 8 summarizes the properties calculated with the procedure described above. Both models tend to the lumped parameters model when the opposite limits are analyzed regarding the cell-substrate height predicted in the best estimate case. Obviously, when this situation is analyzed, the merit function increases to the characteristic value of the lumped parameters model.

From the above analysis, we found two opposite trends. In its limit case, our model reduces to the two-parameters model for lower heights, and the G&K model reduces to the two-parameters model for higher heights, both compared with their best parameter values. Even when this situation is hypothetical (we are not physically changing the height), the G&K model behaves asymptotically as physical interpretation expects it to do: when the cell-substrate height is high enough, the resistance associated to the radial pathway is negligible and the overall response is expected to be well modeled by the lumped parameters model [49].

Even when the analysis presented above puts all models together under the same framework, it is still not clear the reason why this behavior is observed. To understand it, we have to look at the cell-substrate potential, which is defined in both the G&K model and our model. Figure 9 shows the magnitude of this potential normalized to the applied potential as a function of the radial distance, normalized to the cell radius (G&K model) or to the electrode radius (mean-field model), and the logarithm of the frequency, for different

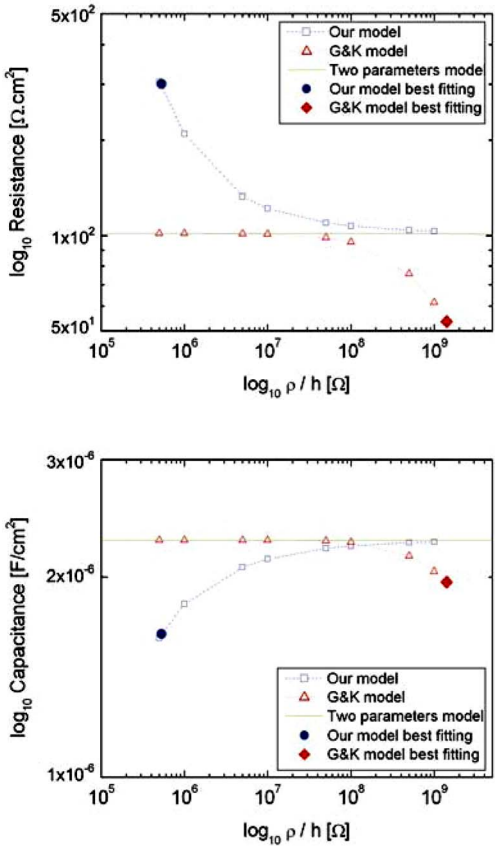

FIG. 8. (Color online) Best estimate of the electrical parameters in G&K model and our model when it is considered a given value for ρ/h. The limiting cases in both models tend to the lumped parameters model.

cases. Figures 9(a) and 9(b) show the potential in our model for its best estimate case ($\rho/h=0.533$ MΩ), and its limit to the lumped parameters case ($\rho/h=1.0$ GΩ), respectively. Figures 9(c) and 9(d) [50] show the same situations where the best estimate case and the limit to the lumped parameters case are defined for the G&K model ($\alpha=26.3\ \Omega^{1/2}$ cm, and $\alpha=0.511\ \Omega^{1/2}$ cm, respectively).

From Figs. 9(b) and 9(d) we can see the key issue in the limit of both differential models to the lumped parameters model. In this limit, given any frequency the potential is flat through the cell or the electrode, so there is no radial gradient in this magnitude. The overall electrical response results from current crossing axially through the system, and it can be modeled by two parameters.

Figures 9(a) and 9(c) show the potentials developed in the best parameters fitting case of the two distributed models considered. Beyond the differences in the expressions that define cell-covered impedance in the two models, which produce the difference in the estimation of the cell-substrate height, and other subtler differences, it is worth noting the close resemblance between these potentials. Both models are strongly influenced by the radial potential [51] and such a likeness means an equivalence between them. The close resemblance is produced by the Bessel functions, which appear in the radial potential in both models. For Bessel functions to produce this shape on the potential, it is necessary that the respective arguments be of the same order. Whichever the argument analyzed, we found a similar structure: a part composed by the radial scale, either r_c in the G&K model or R_e in our model, a part composed by the inverse square root of the axial scale, $(\rho/h)^{1/2}$ in both models, and a part which establishes the direction on the complex plane, given by the impedances in the system. Since the arguments in both models have to be in the same order of magnitude, the difference in the radial scale affects the adjusted scale in the axial direction. The higher radial scale in our model leads to the adjustment process, yielding a higher axial scale than in G&K model, and vice versa. Given an electrode, the problem has two associated radial scales, one microscopic scale given by r_c and one macroscopic given by R_e, so the adjusted height has two values depending on what analysis is considered, and they act as the limits for its estimate. Independent measurements performed by fluorescence interference contrast microscopy [46] give a space of $\sim$50 nm between the basal membrane and the substrate (silicon dioxide). Thus the results obtained with the analysis presented in this paper are consistent with independent measurements of the cell-substrate height.

The above conclusion is obtained when both models are considered independently: each of the models establishes a bound in the cell-substrate height. However, beyond the resemblance in the shapes, Figs. 9(a) and 9(c) also display the same scale in the vertical axis, the normalized potential. Since the normalization is performed with a potential common to both models (the applied potential), the cell-substrate potential has the same order of magnitude whichever model is considered. Remembering that the G&K model does not take into account any macroscopic potential, and our model is based on the assumption that the macroscopic potential is much higher than the microscopic potential, Figs. 9(a) and 9(c) tell us that both effects are important and neither the G&K model nor our model is realistic independently because the potential in the counterpart is important, at least for these measurements. A proper model is still missing, and it should simultaneously consider both effects.

IV. CONCLUDING REMARKS

Much interest is focused on electrical measurements of cells cultured *in vitro*, including experiments where the electrical properties of the cells transduce biological phenomena or evolutions. The ECIS technique appears as a well-grounded technique for this kind of assessment, and models to analyze its data are necessary to produce meaningful information, beyond monitoring the behavior of a single frequency of stimulation. Previous models used to analyze data in electrical measurements were either composed by lumped parameters or resulted exclusively from microscopic considerations. In this paper, we examined a model that, in addition to properly adjusting data generated in ECIS experiments, can correlate in a formal manner the variables estimated from models constructed with the different approaches. One particular measurement currently obtained from ECIS experiments is the cell-substrate height. Our model produces an estimate for this magnitude and its results are extremely dif-

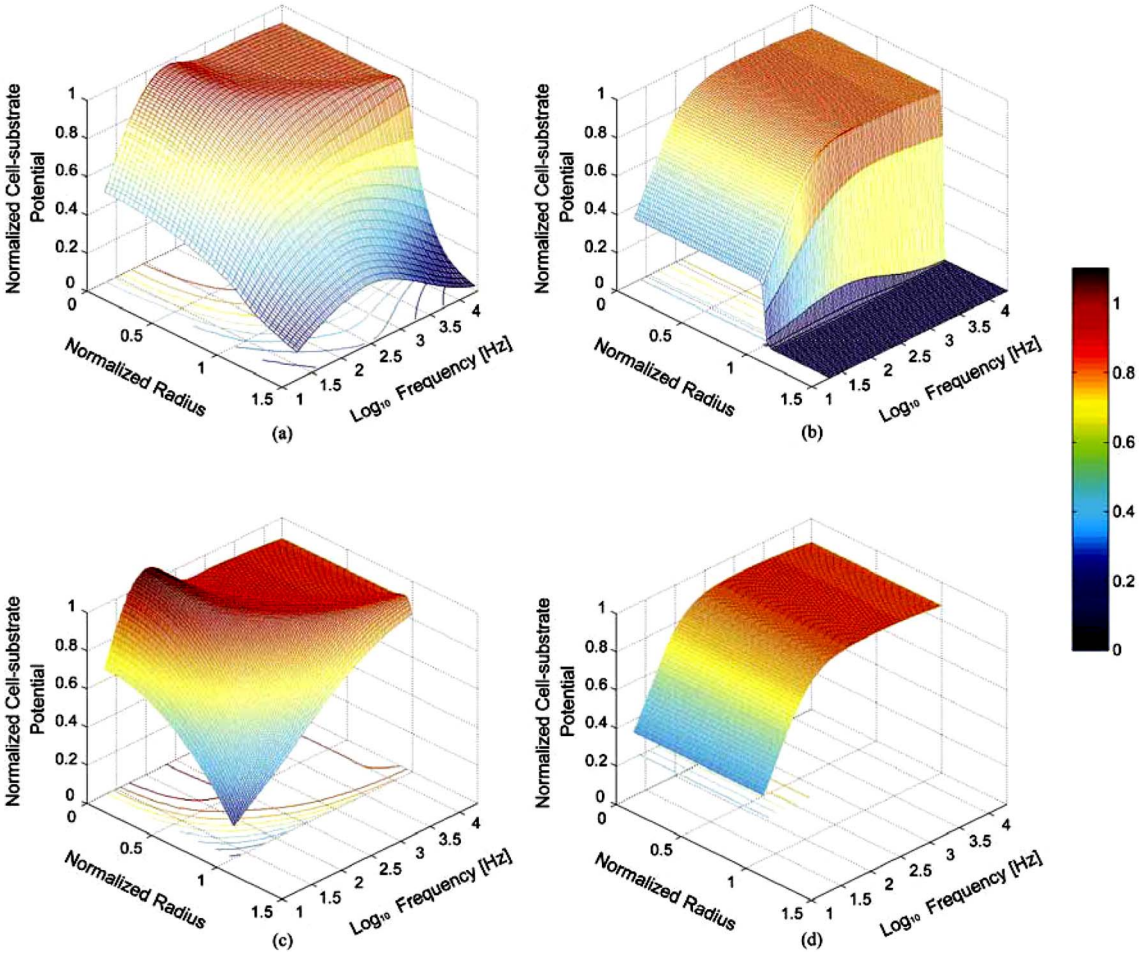

FIG. 9. (Color online) Cell-substrate potential as a function of the distance and the logarithm of frequency, for both the G&K model and the mean-field model, when different cell-substrate heights are considered. Cell-substrate potential, V, is normalized to the applied potential, V_n, and the magnitude of this ratio is considered. In the G&K model, the distance is normalized to the cell radius, whereas in the mean-field model, the distance is normalized to the electrode radius. (a) Mean-field model with height obtained from the best parameters fitting of mean-field model, $\rho/h=0.533$ MΩ. (b) Mean-field model with height obtained from the best parameters fitting of G&K model (limit to lumped parameters case), $\rho/h=1.0$ GΩ. (c) G&K model with height obtained from the best parameters fitting of G&K model, $\alpha=26.3\ \Omega^{1/2}$ cm [50]. (d) G&K model with height obtained from the best parameters fitting of mean-field model (limit to lumped parameters case), $\alpha=0.511\ \Omega^{1/2}$ cm. Potential in mean-field model extends beyond electrode limit (normalized radius=1), whereas potential in G&K model extends up to the cell limit (normalized radius=1).

ferent from those estimated with the Giaever and Keese model. As we show, for a given electrode, values obtained for this magnitude from both models in ECIS experiments should be considered as its limits instead of true values.

ACKNOWLEDGMENTS

We thank M. O. Sonnaillon for technical support and useful comments. E.U. was partially supported by INVAP S.E.

[1] R. I. Freshney, *Culture of Animal Cells*, 3rd ed. (Wiley-Liss, New York, 1994).
[2] I. Giaever and C. R. Keese, Proc. Natl. Acad. Sci. U.S.A. **81**, 3761 (1984).
[3] I. Giaever and C. R. Keese, IEEE Trans. Biomed. Eng. **33**(2), 242 (1986).
[4] C. R. Keese and I. Giaever, IEEE Eng. Med. Biol. Mag. **13**(3), 402 (1994).
[5] I. Giaever and C. R. Keese, Nature **366**, 591 (1993).
[6] J. Wegener, C. R. Keese, and I. Giaever, Exp. Cell Res. **259**, 158 (2000).
[7] I. Giaever and C. R. Keese, Proc. Natl. Acad. Sci. U.S.A. **88**, 7896 (1991).
[8] C.-M. Lo, C. R. Keese, and I. Giaever, Exp. Cell Res. **204**, 102 (1993).
[9] I. Giaever and C. R. Keese, CHEMTECH **22**, 116 (1992).

[10] C. R. Keese, N. Karra, B. Dillon, A. M. Goldberg, and I. Giaever, In vitro Mol. Toxicol. **11**(2), 183 (1998).
[11] S. Arndt, J. Seebach, K. Psathaki, H.-J. Galla, and J. Wegener, Biosens. Bioelectron. **19**, 583 (2004).
[12] L. Reddy, H.-S. Wang, C. R. Keese, I. Giaever, and T. J. Smith, Exp. Cell Res. **245**, 360 (1998).
[13] J. Wegener, S. Zink, P. Rösen, and H.-J. Galla, Eur. J. Physiol. **437**, 925 (1999).
[14] C. Tiruppathi, W. Yan, R. Sandoval, T. Naqvi, A. N. Pronin, J. L. Benovic, and A. B. Malik, Proc. Natl. Acad. Sci. U.S.A. **97**, 7440 (2000).
[15] B. F. DeBlasio, J.-A. Røttingen, K. L. Sand, I. Giaever, and J.-G. Iversen, Acta Physiol. Scand. **180**, 335 (2004).
[16] C. Tiruppathi, A. B. Malik, P. J. DelVecchio, C. R. Keese, and I. Giaever, Proc. Natl. Acad. Sci. U.S.A. **89**, 7919 (1992).
[17] C.-M. Lo, C. R. Keese, and I. Giaever, Exp. Cell Res. **250**, 576 (1999).
[18] J. Wegener, A. Hakvoort, and H.-J. Galla, Brain Res. **853**, 115 (2000).
[19] N. Kataoka, K. Iwaki, K. Hashimoto, S. Mochizuki, Y. Ogasawara, M. Sato, K. Tsujioka, and F. Kajiya, Proc. Natl. Acad. Sci. U.S.A. **99**, 15638 (2002).
[20] C. R. Keese, K. Bhawe, J. Wegener, and I. Giaever, BioTechniques **33**, 842 (2002).
[21] C.-M. Lo, C. R. Keese, and I. Giaever, Exp. Cell Res. **213**, 391 (1994).
[22] C.-M. Lo, M. Glogauer, M. Rossi, and J. Ferrier, Eur. Biophys. J. **27**, 9 (1998).
[23] C.-M. Lo and J. Ferrier, Eur. Biophys. J. **28**, 112 (1999).
[24] T. J. Smith, H.-S. Wang, M. G. Hogg, R. C. Henrikson, C. R. Keese, and I. Giaever, Proc. Natl. Acad. Sci. U.S.A. **91**, 5094 (1994).
[25] J. Wegener, C. R. Keese, and I. Giaever, BioTechniques **33**, 348 (2002).
[26] C. R. Keese, J. Wegener, S. R. Walker, and I. Giaever, Proc. Natl. Acad. Sci. U.S.A. **101**, 1554 (2004).
[27] For further references about the studies carried out under ECIS technique, see www.biophysics.com
[28] D. A. Borkholder, Ph.D. thesis, Stanford University, 1998 (unpublished).
[29] E. Gileadi, *Electrode Kinetics for Chemists, Chemical Engineers and Materials Scientists* (Wiley-VCH, New York, 1993).
[30] E. T. McAdams, A. Lackermeier, J. A. McLaughlin, D. Macken, and J. Jossinet, Biosens. Bioelectron. **10**, 67 (1995).
[31] J. Wegener, M. Sieber, and H.-J. Galla, J. Biochem. Biophys. Methods **32**, 151 (1996).
[32] T. G. Păunescu and S. I. Helman, Biophys. J. **81**, 838 (2001).
[33] C. A. Bertrand, D. M. Durand, G. M. Saidel, C. Laboisse, and U. Hopfer, Biophys. J. **75**, 2743 (1998).
[34] C. Clausen, S. A. Lewis, and J. M. Diamond, Biophys. J. **26**, 291 (1979).
[35] C.-M. Lo, C. R. Keese, and I. Giaever, Biophys. J. **69**, 2800 (1995).
[36] C.-M. Lo and J. Ferrier, Phys. Rev. E **57**, 6982 (1998).
[37] The impedance of the naked electrode takes into account all the metal-electrolyte phenomena, and it is supposed to remain invariable even when cells are attached to the surface. Independence of this property on current densities is implicit to this assumption.
[38] As the whole response is not only defined within the electrode area, the normalization of the impedances by this magnitude is not straightforward. However, we prefer to do so, instead of working with non-specific impedances, because posterior expressions are simple.
[39] A better description for the impedance of the monolayer, $Z_{cells}(\omega)$, could be achieved in different ways: for example, recognizing intercellular and paracellular resistive pathways, working with the geometry of one cell and the different impedance contributions, etc. However, any improvement in the description results in a more complex model (more parameters) and the comparison with the existing models would not be under equal basis.
[40] M. O. Sonnaillon and F. J. Bonetto, Rev. Sci. Instrum. **76**, 024703 (2005).
[41] Due to limitations of the DSP unit, the superior limit of the frequencies analyzed was fixed at 20 kHz. However, this is not a limitation for the analysis because most of the electrical information can be obtained from data below it.
[42] D. W. Marquardt, J. Soc. Ind. Appl. Math. **11**, 431 (1963).
[43] The aim of this procedure was to keep only real numbers in the minimization routines.
[44] The spread resistance dominates the in-series resistance of the system at high frequencies. Normally it is not considered as belonging to the electrode-electrolyte interface, and it is in-series with it.
[45] This situation is not general because we can always change the assumption about Z_{cells} or consider a fixed C_m in the G&K model, for instance.
[46] D. Braun and P. Fromherz, Biophys. J. **87**, 1351 (2004).
[47] If the mean-field model would consider a more realistic description for the impedance of the monolayer [39], the value for the cell-substrate height will probably be closer to that obtained by Ref. [46]. However, the discrepancy described here takes into account the deficiency in the modeling of *equivalent* models.
[48] Normalized properties are obtained dividing by the corresponding property of the naked electrode response.
[49] However, since this contribution is not only defined by the resistance but also by the current flowing radially through this interspace (and this variable is coupled with the all the other variables and properties), we cannot conclude that our model is not correct, although it behaves in a nonintuitive way.
[50] In Fig. 9(c) there is a region where normalized potential exceeds 1. Apparently striking at first sight, this situation is possible since radial and applied potentials relate with the derivative of the applied current.
[51] In both models, radial potential appears in all differential equations, except in the expression for the conservation of the current.